

Gene Expression and Transcriptome Profiling of Changes in a Cancer Cell Line Post-Exposure to Cadmium Telluride Quantum Dots: Possible Implications in Oncogenesis

Dose-Response:
An International Journal
April-June 2021:1-18
© The Author(s) 2021
Article reuse guidelines:
sagepub.com/journals-permissions
DOI: 10.1177/15593258211019880
journals.sagepub.com/home/dos



Mohammed S. Aldughaim¹, Mashael R. Al-Anazi², Marie Fe F. Bohol² ,
Dilek Colak³ , Hani Alotheid⁴ , Salma Majid Wakil⁵, Samya T. Hagos⁵,
Daoud Ali⁶, Saud Alarifi⁶ , Sashmita Rout⁷, Saad Alkahtani⁶,
Mohammed N. Al-Ahdal^{2,8}, and Ahmed A. Al-Qahtani^{2,8}

Abstract

Cadmium telluride quantum dots (CdTe-QDs) are acquiring great interest in terms of their applications in biomedical sciences. Despite earlier sporadic studies on possible oncogenic roles and anticancer properties of CdTe-QDs, there is limited information regarding the oncogenic potential of CdTe-QDs in cancer progression. Here, we investigated the oncogenic effects of CdTe-QDs on the gene expression profiles of Chang cancer cells. Chang cancer cells were treated with 2 different doses of CdTe-QDs (10 and 25 µg/ml) at different time intervals (6, 12, and 24 h). Functional annotations helped identify the gene expression profile in terms of its biological process, canonical pathways, and gene interaction networks activated. It was found that the gene expression profiles varied in a time and dose-dependent manner. Validation of transcriptional changes of several genes through quantitative PCR showed that several genes upregulated by CdTe-QD exposure were somewhat linked with oncogenesis. CdTe-QD-triggered functional pathways that appear to associate with gene expression, cell proliferation, migration, adhesion, cell-cycle progression, signal transduction, and metabolism. Overall, CdTe-QD exposure led to changes in the gene expression profiles of the Chang cancer cells, highlighting that this nanoparticle can further drive oncogenesis and cancer progression, a finding that indicates the merit of immediate *in vivo* investigation.

Keywords

Quantum dots, nanocrystals, microarray, tumorigenesis, nanotoxicity, CdTe-QDs

¹ Research Centre, King Fahad Medical City, Riyadh, Saudi Arabia

² Department of Infection and Immunity, Research Centre, King Faisal Specialist Hospital & Research Centre, Riyadh, Saudi Arabia

³ Department of Biostatistics, Epidemiology and Scientific Computing, Research Centre, King Faisal Specialist Hospital & Research Centre, Riyadh, Saudi Arabia

⁴ Department of Basic Medical Sciences, Faculty of Applied Medical Sciences, Al-Baha University, Al-Baha, Saudi Arabia

⁵ Genotyping Core Facility, Research Centre, King Faisal Specialist Hospital & Research Centre, Riyadh, Saudi Arabia

⁶ Department of Zoology, College of Science, King Saud University, Riyadh, Saudi Arabia

⁷ Advanced Centre for Treatment, Research, and Education in Cancer, Tata Memorial Hospital, Mumbai, India

⁸ Department of Microbiology and Immunology, Alfaisal University, School of Medicine, Riyadh, Saudi Arabia

Received 28 March 2021; received revised 28 April 2021; accepted 30 April 2021

Corresponding Author:

Ahmed A. Al-Qahtani, Department of Infection and Immunity, Research Centre, King Faisal Specialist Hospital & Research Centre, Makkah Al Mukarramah Branch Road, Al Madhar Ash Shamali, Riyadh 11211, Saudi Arabia.

Email: aqahtani@kfshrc.edu.sa



Creative Commons Non Commercial CC BY-NC: This article is distributed under the terms of the Creative Commons Attribution-NonCommercial 4.0 License (<https://creativecommons.org/licenses/by-nc/4.0/>) which permits non-commercial use, reproduction and distribution of the work without further permission provided the original work is attributed as specified on the SAGE and Open Access pages (<https://us.sagepub.com/en-us/nam/open-access-at-sage>).

Introduction

Quantum dots (QDs) are colloidal and fluorescence-based semiconductor nanocrystals, which have been studied as a novel probe for biomedical applications both *in vitro* and *in vivo*, due to their unique optical and electronic properties.¹ QDs contain elements from groups II to VI or III to V and are composed of clusters of cadmium selenide, cadmium sulphide, indium arsenide, or indium phosphide (2-10 nm in diameter). Their unique properties include wide and continuous absorption spectra, narrow emission spectra, and high light stability.¹ In addition to their use in solar cells and light-emitting devices (LEDs), QDs have attracted great interest in biomedical applications for multiple colour imaging and targeted drug delivery.^{2,3} Although QDs have excellent diagnostic and therapeutic potential, considerable fluorescence loss following injection into tissues/organs has been reported due to degradation of coated surface ligands or dyes absorbed to the surface when subjected to the presence of body fluids.⁴

The associated cytotoxicity of QDs that influences cell growth and viability, depending on size, capping materials, surface chemistry, and coating bioactivity, has also been reported.⁵ Due to the ease of production in their aqueous phase, cadmium telluride QDs (CdTe-QDs) are the most frequently used.^{6,7} However, the potential toxicity of CdTe-QDs to human health following exposure to the particle stems from their particle size, heavy metal formulation, concentration, and duration of exposure. Additionally, the cytotoxic mechanisms of CdTe-QDs include desorption of free QD core upon degradation, and free radical formation, the interaction of QDs with intracellular components and pathways, and generation of reactive oxygen species (ROS).⁷ It should also be noted here that small-diameter CdTe-QDs (2 nm) are more toxic than large CdTe-QDs (5 nm). Findings from previous studies indicate that CdTe-QD exposure to human hepatocellular carcinoma HepG2 cells causes enhanced levels of ROS, together with apoptotic induction characterized by altered levels of caspase 3, poly ADP-ribose polymerase (PARP) cleavage, and externalization of phosphatidylserine (PS) via extrinsic pathways (as evident from increased Fas and caspase 8 levels). In addition, rats exposed to 3-mercaptopropionic acid (MPA)-modified CdTe-QDs showed impaired spatial learning and memory, involving PI3K-Akt and MPAK-ERK signaling pathways.^{8,9} A further finding is that CdTe-QDs induce apoptosis in human breast cancer cells via ROS generation.¹⁰ They can also reduce viability and motility in mice spermatozoa,¹¹ and their exposure to *Hydra vulgaris* – an invertebrate model – induces chromosomal fragmentation.¹² The potential carcinogenic effect of CdTe QDs in normal human bronchial epithelial cells has also been documented.¹³

Nanoparticles with cytotoxic effects have been widely investigated for potential anticancer properties.¹⁴ Unfortunately, some of these nanoparticles may induce their cytotoxic effect on normal cells, or even drive cancer progression.^{15,16} In the same manner, nanoparticles, such as CdTe QDs that have diagnostic potential, may exhibit similar negative properties,

and there have been reports of the cytotoxic potential of CdTe QDs on cancer cells.¹⁷ As such, it is pertinent to investigate the mechanisms of QD cytotoxicity. Indeed, to assess the global effect of nanoparticles on target cells, transcriptomic profiling has been undertaken in several studies, as in the case of silver and titanium nanoparticles,¹⁸ genotoxic and non-genotoxic carcinogens,¹⁹ 11-nm dimercaptosuccinic acid-coated magnetite nanoparticles,²⁰ and for fibroblasts.²¹

The aim of this study is thus to investigate the effects of CdTe-QD exposure in Chang cancer cells via microarray gene expression profiling to explore their oncogenic potential in terms of causing a more aggressive form of cancer. In addition, we aim to identify the pathways and networks associated with the differential gene expression in CdTe-QD-exposed cancer cells.

Materials and Methods

Characterization of CdTe QDs

CdTe QDs were procured from Nano Impex (Mississauga, Ontario, Canada); the characterization of CdTe QDs nanocrystals has been previously reported.²² Nanocrystals were suspended in a culture medium at a concentration of 1 mg/mL and sonicated using a Branson sonifier (Branson Ultrasonics, Danbury, CT, USA) at 40 W for 15 min before use.

Cell Culture

Human Chang cancer cells line were grown in Dulbecco's modified Eagle's medium (DMEM) (Gibco-BRL, Grand Island, NY, USA) supplemented with 10% fetal bovine serum (FBS) (HyClone Laboratories, Logan, UT) and antibiotics (100 IU/mL penicillin, 100 µg/mL streptomycin). The cells were incubated at 37°C and 5% v/v CO₂ until 80% confluence was achieved.

Treatment of Cells with CdTe-QDs

Chang cancer cells were exposed to varying concentrations of CdTe-QDs at different time points. Firstly, the cells (1×10^5 cells/well) were seeded into 24-well plates and incubated until the optimal confluence was reached. After washing with Phosphate Buffered Saline (PBS) (Fisher BioReagents), the cells were then placed in a fresh growth media, containing either 10 µg/mL or 25 µg/mL of CdTe-QDs, and further incubated for 6 h, 12 h and 24 h at each concentration.

Microarray Analysis

The total RNA content of the exposed Chang cancer cells was extracted using QIAamp RNA Blood Mini Kit (Qiagen, Hilden, Germany) following the manufacturer's instructions. The integrity of the extracted RNA was determined using the *Agilent Bioanalyzer 2100* system (*Agilent* Technologies, Santa Clara, CA, USA). For microarray analysis, cDNA synthesis of the total RNA was first performed. Briefly, cDNA synthesis of

the total RNA was transcribed using a High-Capacity cDNA Reverse Transcription Kit (Applied Biosystems, Foster City, CA, USA). The obtained cDNA was subsequently used for *in vitro* analysis of global gene transcription, using GeneChip (Affymetrix, Santa Clara, CA, USA) following the manufacturer's instructions. To analyze the global gene expression profile, generated fluorescent oligonucleotide probes were hybridized to the GeneChips[®] Human Genome HG-U133 Array in a GeneChip[®] hybridization oven, as per the standard instructions of the manufacturer. This array contained nearly 55,000 probe sets, representing over 39,000 transcripts from 33,000 previously identified human genes. Post-hybridization washing and staining were performed with a GeneChip[®] Fluidics Station 400 (Affymetrix). Subsequently, findings were visualized using a Gene Array scanner (Affymetrix). For image quantitation, GeneChip[®] Operating Software was utilized.

Data normalization was performed using the GC Robust Multi-array Average (GC-RMA) algorithm. Significantly regulated genes for different doses (10 μg and 25 μg) at the three-time points (6 h, 12 h, and 24 h) were determined using 2-factor analysis of variance (ANOVA) by including dosage, time, and their interactions in the statistical model. Genes exhibiting false discovery rate (FDR)-adjusted P -value < 0.05 and the absolute fold changes (FC) > 2 in treated cells as compared with those of the control cells were considered significant. Statistical analysis was conducted with the PARTEK Genomics Suite (Partek Inc., St. Lois, MO, USA).

Quantitative RT-PCR Validation of Microarray Gene Expression

To validate the microarray analysis, selected genes that were significantly and differentially expressed in the microarray analysis were individually tested via qRT-PCR. Isolated RNA was treated with DNase I (Promega, Madison, USA), and cDNA was synthesized using All-in-One cDNA Synthesis SuperMix (Biotool, Houston, USA). Primers and probes for the target genes were purchased from Applied Biosystems (Foster City, California, USA). A Taqman Universal qPCR Master Mix (Applied Biosystems) was then used, and the amplification reaction was set up using the Applied Biosystems 7900HT Fast Real-Time PCR System.

The cycling parameters were as follows: 5 min at 90-95°C, 40 cycles of 30 s at 95°C, and 45 s at 60°C. The fold-changes of the specific RNA transcripts were calculated using the ΔCt method, and the mRNA expression levels of studied genes were then normalized to GAPDH. The final data for qRT-PCR were described as mean \pm standard deviation (SD) change relative to the untreated cells.

Functional Pathway, Upstream Regulator, and Network Analysis

Functional, pathway and gene ontology (GO) enrichment analyses were performed using the Database for Annotation, Visualization and Integrated Discovery (DAVID), Protein Analysis

Through Evolutionary Relationships (PANTHER[™]) classification systems, and Ingenuity Pathways Analysis (IPA) (QIAGEN Inc., <https://www.qiagenbioinformatics.com/products/ingenuity-pathway-analysis>). We also performed canonical pathways and gene network analysis using IPA. The DEGs lists for each concentration for different time points were mapped to their corresponding gene object in the Ingenuity Pathway Knowledge Base and protein-protein interaction networks. A right-tailed Fisher's exact test was used to calculate a P -value, determining the probability that the biological function (or pathway) assigned to that data set can be explained by chance alone, based on the functional/pathway annotations stored in the Ingenuity Knowledge Base. All statistical tests were 2-sided and a P -value < 0.05 was considered statistically significant.

Results:

CdTe QD Exposure Induced Differential Expression of Potentially Oncogenic Genes

Microarray analysis revealed that CdTe-QD-exposed Chang cancer cells triggered differential expressions of various genes, with a possible contribution to oncogenesis. CdTe-QD (10 $\mu\text{g}/\text{ml}$) treatment led to the identification of a total of 1891 DEGs at 6 h, 12 h, and 24 h, resulting in 1072, 972, and 27 DEGs respectively (Figure 1A). However, a considerably higher number of DEGs (10,575) were detected in cells exposed to 25 $\mu\text{g}/\text{mL}$ CdTe-QDs at all time points. These included 1089, 7644, and 5773 DEGs at 6 h, 12 h, and 24 h respectively (Figure 1B). The genes and pathways identified in each treatment group are summarized in Supplementary Tables (1-6). Fold changes were seen in the case of several genes, which are associated with cell cycle regulation and signal transduction.

Cluster Analysis of CdTe-QD Sensitive Genes

Venn diagrams were generated to analyze the specific and common genes triggered as a result of CdTe-QD exposures (10 and 25 $\mu\text{g}/\text{ml}$) at different time points. Treatments with 10 $\mu\text{g}/\text{mL}$ of CdTe-QDs revealed that 7 genes were either commonly upregulated or suppressed at all the time points tested (6 h, 12 h, and 24 h) (Figure 1A). The heat map of DEGs observed at 10 $\mu\text{g}/\text{mL}$ of CdTe-QDs (Figure 2A) shows the expression levels of various genes that were upregulated (red) and suppressed (green) within the $-3.0 \sim 3.0$ range. The y-axis of the heat map shows the corresponding most-associated GO for biological processes (Figure 2A). Genes associated with transcription, post-transcriptional modifications, cell cycle, anion transport, and homeostasis were highly expressed in the unexposed control cells (0 $\mu\text{g}/\text{ml}$; 0 h) and in cells treated with 10 $\mu\text{g}/\text{mL}$ of CdTe-QDs at 0 h, and this expression was maintained in the controlled unexposed cells until the 24 h point. However, in cells exposed to 10 $\mu\text{g}/\text{mL}$ CdTe-QD, the expression of the set of genes remained high at 6 h, and a suppression in the expression of these genes was observed at 12 h. This later

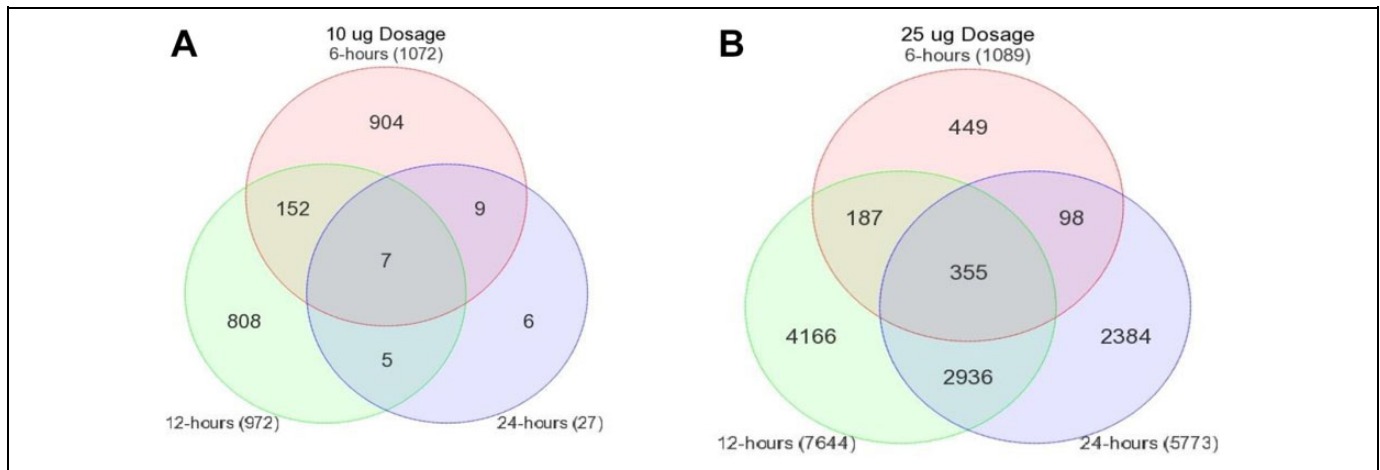


Figure 1. Venn diagrams representing the differentially expressed genes specific or common to different time points in 10 µg (A) and 25 µg (B). Microarray analysis revealed that CdTe-QDs treated Chang cancer cells triggered differential expressions of various genes (DEGs). CdTe-QDs (10 µg/mL) treatment revealed 1891 DEGs at 6 h, 12 h, and 24 h, resulting in 1072, 972 and 27 DEGs respectively (A). A higher number of DEGs (10,575) were detected with 25 µg/mL CdTe-QD. This included 1089, 7644 and 5773 DEGs at 6 h, 12 h and 24 h respectively (B). Venn diagrams were generated to determine the possible outcome of specific and common genes triggered as a result of CdTe-QDs treatments (10 and 25 µg/mL) at different time points.

increased at 24 h. In the same manner, genes involved in developmental processes, organelle organization, cell adhesion, and signal transduction were also highly expressed in unexposed control cells, and the CdTe-QD-exposed cells at 0 h were weakly expressed at 6 h in the CdTe-QD-exposed cells. Furthermore, the expression of these sets of genes was further reduced at 12 h and 24 h in the low-dose (10 µg/mL) CdTe-QD-exposed cells. The genes involved with the GO of processes of metabolism, cellular organization, and protein organization exhibited a lower expression level in the controls, but higher expression level in the cells exposed to low-dose CdTe-QDs until the 6 h point. However, after 12 h and 24 h exposure, the expression of these genes reduced to a moderate level.

Hierarchical clustering analysis revealed that the DEGs expressed in response to low-doses of CdTe-QDs were classified into four groups based on the time of exposures of 0 h, 6 h, 12 h, and 24 h. We observed that the gene expression pattern of cells at 24 h was similar to the control (0 h), whereas 6 h and 12 h exposure showed more diverse and unique expression patterns (Figure 2A). We performed a similar analysis for the DEGs in the cancer cells exposed to the high dose (25 µg/ml) of CdTe-QDs across the time points 6 h, 12 h, and 24 h. As shown in the Venn diagram in Figure 1B, 355 unique DEGs were identified each at 6 h, 12 h, and 24 h time points in the high-dose treatment. Figure 2B also illustrates the heat map of DEGs induced or repressed for this treatment group (25 µg/ml CdTe-QDs) at the time points investigated. The heat map of DEGs in response to this high dose of CdTe-QDs showed genes associated with GO processes of negative regulation of apoptotic process and mesoderm development to be most highly expressed in controls, followed by the CdTe-QD high-dose exposure group of 6 h, while the expression was further reduced at the 12 h time point. These expression levels were

found to have reduced in the cells treated with the higher dose of CdTe-QDs at 24 h. The genes involved in metabolism, protein modification, transport, localization, and fatty acid beta-oxidation were highly expressed in the unexposed cells, and in the high-dose CdTe-QD-exposed cancer cells at 6 h. These genes were downregulated in the cells exposed to CdTe-QDs at 12 h, and their expressions were comparatively weak at 24 h. In addition, after 6 h and 12 h exposure to high-dose treatment group of cells, the unexposed cells showed much lower expression of genes linked to metabolite production, glycolysis, chromatin organization and nuclear transport. These genes were strongly expressed in the cells treated for 24 h with the high dose of CdTe-QDs. Chang cells exposed to the high dose of CdTe-QDs and incubated for 12 h exhibited increased expression of several genes associated with transcription, post-transcriptional mRNA processing, and cell cycle regulation. However, the expression of these genes was downregulated at 6 h, 24 h, and in the unexposed control cells (Figure 2B). In the hierarchical clustering analysis for high-dose CdTe-QD treatment, we observed the resulting DEGs forming four clusters based on different time durations of exposure. The DEGs also exhibited induced or suppressed expression in the exposed cells at the 6 h point compared to the gene expression patterns for each of the time durations of 12 h and 24 h, both of which were distinctive (Figure 2B).

Gene Ontology Analysis of CdTe-QD-Responsive Genes

We performed enrichment analysis of gene ontology to determine the possible role of the DEGs in the Chang cancer cells treated with different doses of CdTe-QDs for varying time durations. Figure 3A shows the 11 GO categories of biological processes that were significantly upregulated ($P < 0.05$) in the

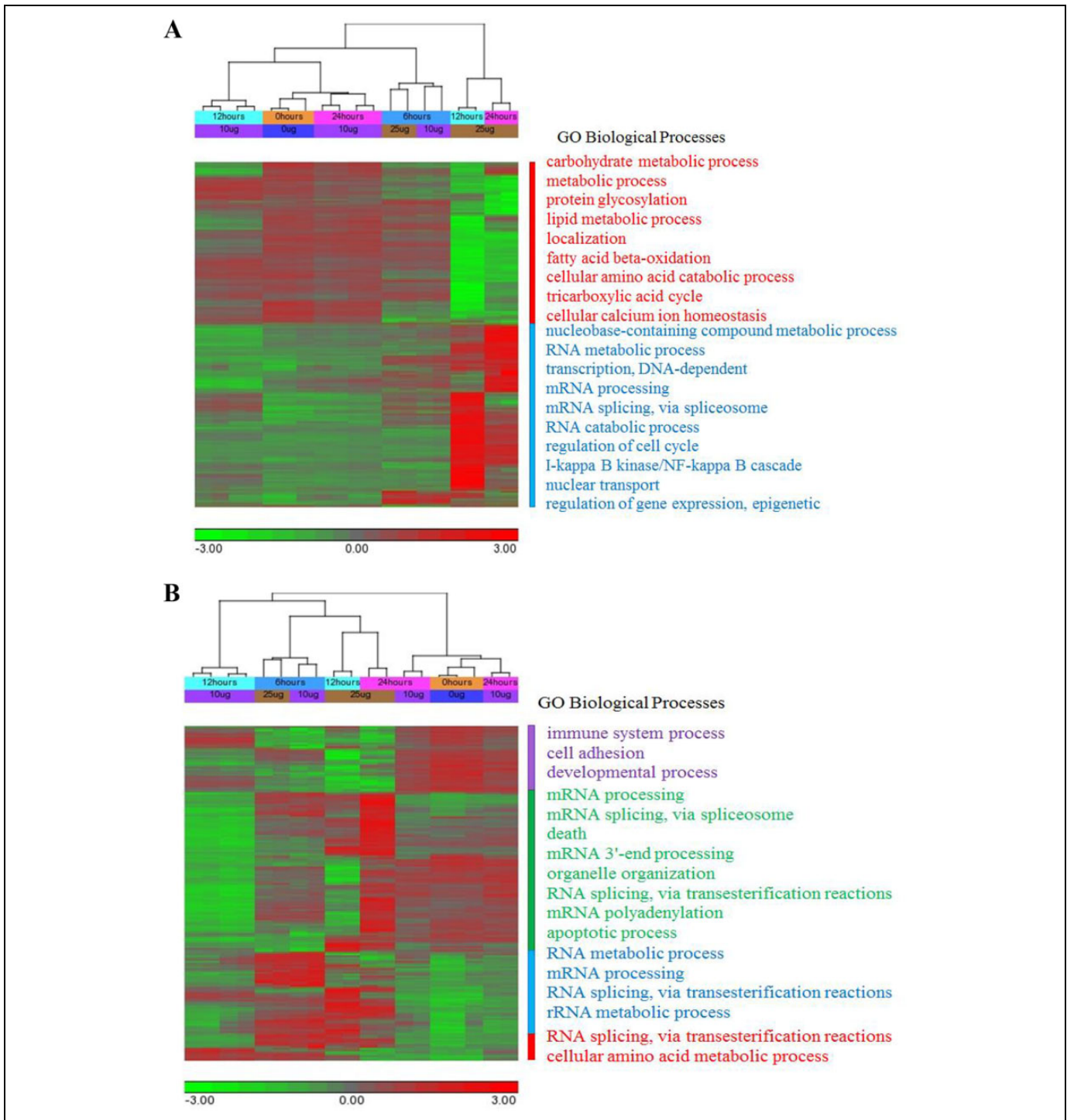


Figure 2. Heat maps of union of DEGs at 10 μg (**A**) and 25 μg (**B**). Hierarchical clustering clearly separated genes into several clusters, revealing the most-associated GO biological processes for each cluster of genes. Red and green denote highly and weakly expressed genes, respectively, within the -3.0~3.0 range. The y-axis of the heat map shows the corresponding most-associated GO biological processes. At 10 μg , the genes associated with RNA splicing showed greater expression while expression of genes involved in mRNA processing and splicing, apoptosis and mRNA polyadenylation were reduced sequentially at 24 h and 12 h with low-dose CdTe-QDs. (**A**). At 25 μg , the genes involved in lipid and carbohydrate metabolism were highly expressed (**B**).

cells treated with 10 $\mu\text{g}/\text{mL}$ of CdTe-QDs at 6 h. These include organismal, cellular, and tissue development, gene expression, cellular movement, growth and proliferation, cell death and

survival, cancer and reproductive system diseases, and organismal survival. The GO analysis for the cells treated with 25 $\mu\text{g}/\text{mL}$ CdTe-QDs for 6 h revealed that cancer; reproductive

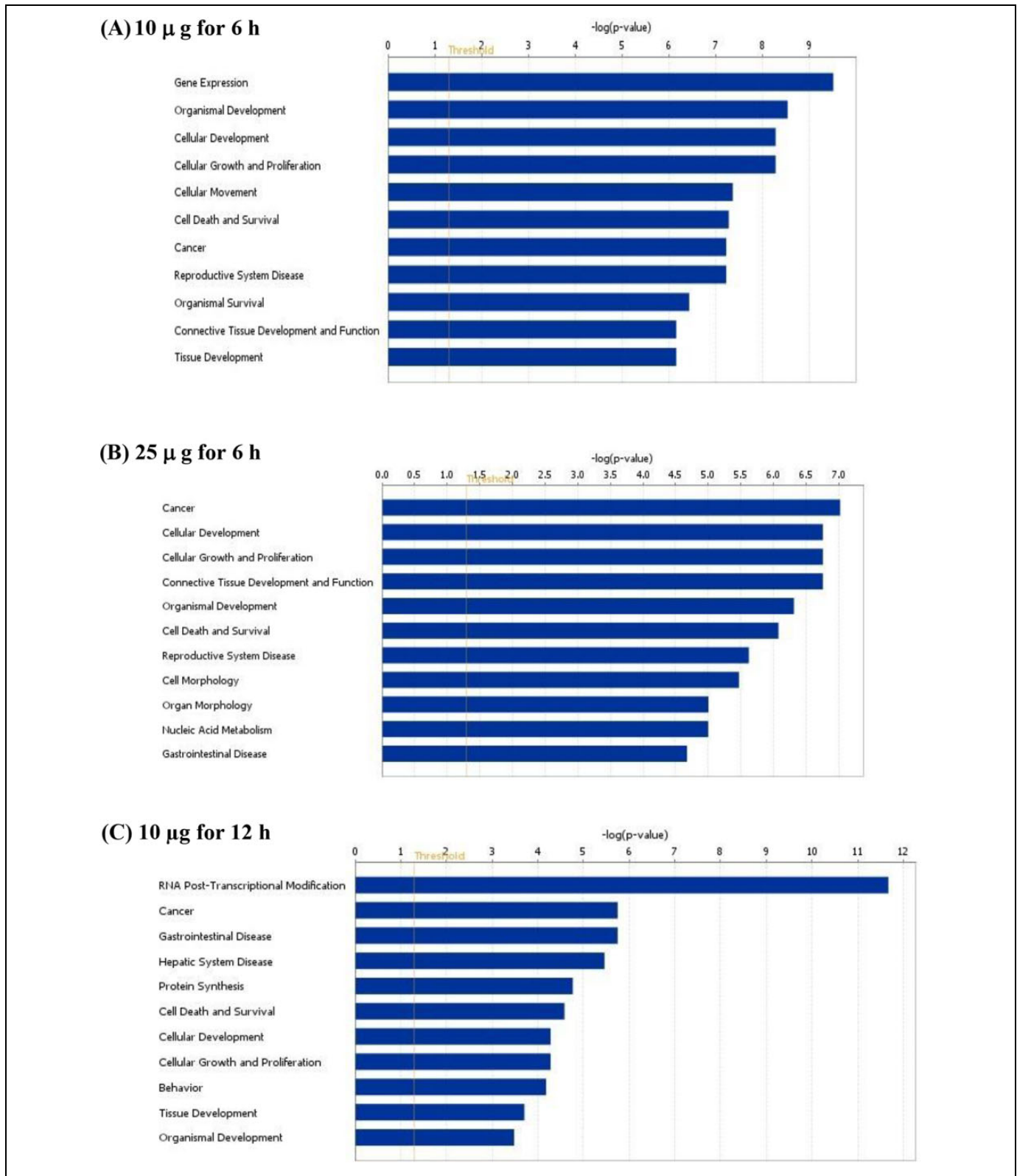


Figure 3. Gene ontology of DEGs significant at 10 μ g and 25 μ g at 6 h. The X-axis indicates the significance ($-\log_{10}(P\text{-value})$). 11 GO categories of biological processes were significantly upregulated ($P < 0.05$) in cells treated with 10 μ g/mL of CdTe-QDs at 6 h (A). GO analysis for the cells treated with 25 μ g/mL CdTe-QDs for 6 h revealed that cancer; reproductive system and gastro-intestinal diseases; cellular development, growth and proliferation; organismal development; connective tissue development and function; cell death and survival, cell and organ morphology; and nucleic acid metabolism responses were significantly affected (B). 10 μ g/mL CdTe-QDs at 12 h identified processes including RNA post-transcriptional modification; cancer; gastrointestinal and hepatic diseases; tissue, cellular, organismal development; cell death and survival; cellular development, growth and proliferation; protein synthesis; and behaviour responses (C),

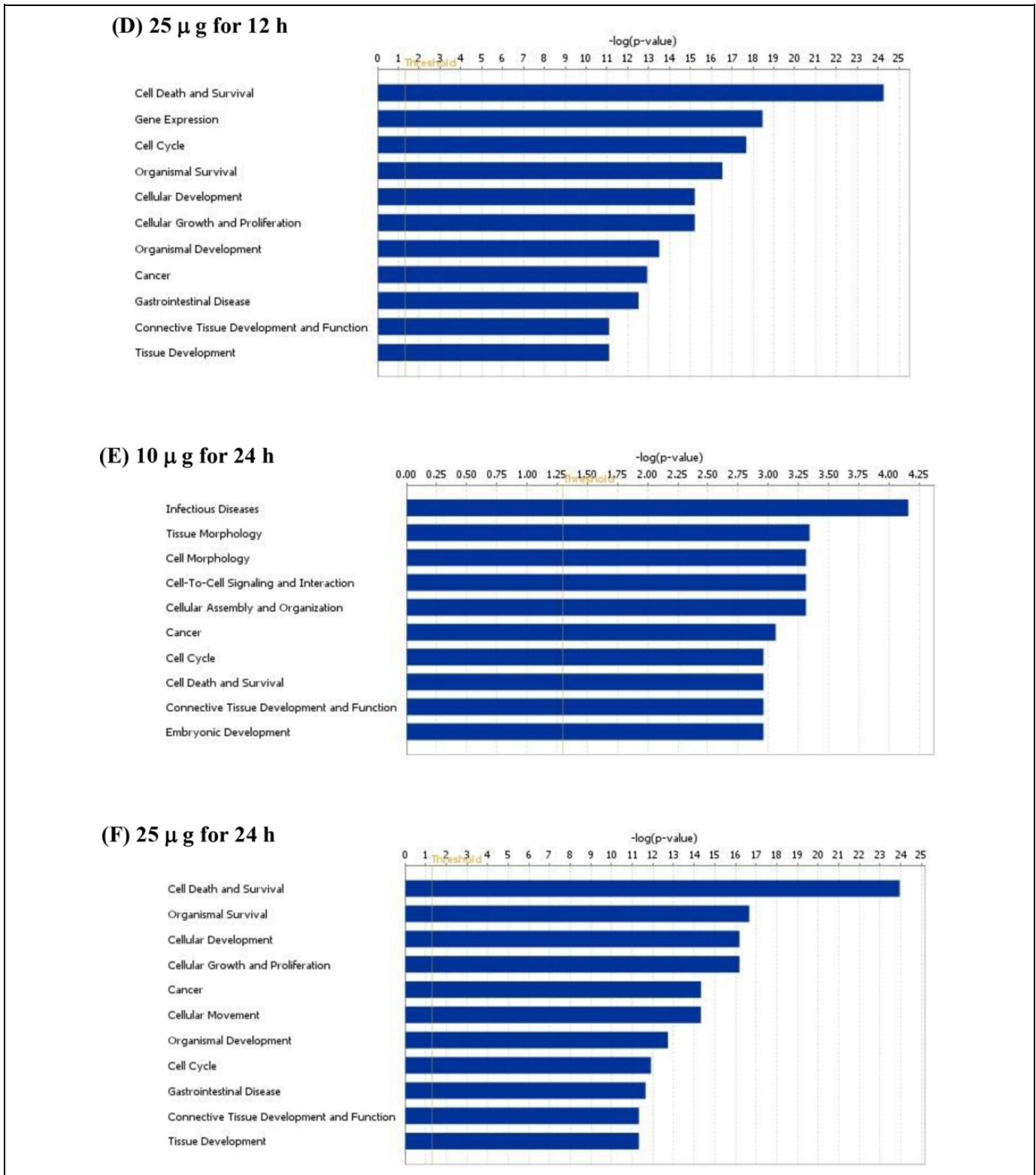


Figure 3. (continued). while 25 μ g/mL CdTe-QD for 12 h revealed pathways involved in cell death and survival; cell cycle; cellular, tissue and organismal development; gene expression; organismal survival; cellular growth and proliferation; cancer and gastro-intestinal diseases; and connective tissue development (**D**). For 10 μ g/mL CdTe-QDs at 24 h, genes pertaining to infectious diseases; tissue and cell morphology; cell-to-cell signaling and interaction; cellular assembly and organization; cancer; cell cycle; cell death and survival; connective tissue development and function; and embryonic development processes were the highlights (**E**). For 25 μ g/mL CdTe-QDs at 24 h, gene expression was associated with cell death and survival; organismal survival; cellular, tissue and organismal development; cellular growth and proliferation; cancer and gastro-intestinal diseases; cellular movement; cell cycle and connective tissue development (**F**).

system and gastro-intestinal diseases; cellular development, growth, and proliferation; organismal development; connective tissue development and function; cell death and survival; cell and organ morphology; and nucleic acid metabolism responses were all significantly affected (Figure 3B). Similar analysis on the cells treated with 10 µg/mL CdTe-QDs for 12 h showed genes responsible for RNA post-transcriptional modification; cancer, gastrointestinal and hepatic diseases; tissue, cellular and organismal development; cell death and survival; cellular development, growth, and proliferation; protein synthesis; and behaviour responses were significantly induced (Figure 3C). Figure 3D demonstrates that expression of genes responsible for biological processes, including cell death and survival; cell cycle; cellular, tissue, and organismal development; gene expression; organismal survival; cellular growth and proliferation; cancer and gastro-intestinal diseases; and connective tissue development and function were significantly enhanced in Chang cancer cells exposed to 25 µg/mL CdTe-QDs for 12 h. In cells treated with 10 µg/mL CdTe-QDs for 24 h, the GO analysis associated the responsive genes with infectious diseases; tissue and cell morphology; cell-to-cell signaling and interaction; cellular assembly and organization; cancer; cell cycle; cell death and survival; connective tissue development and function; and embryonic development processes (Figure 3E). Further analysis of the cells treated with 25 µg/mL CdTe-QDs for 24 h revealed significant induction of genes responsible for cell death and survival; organismal survival; cellular, tissue and organismal development; cellular growth and proliferation; cancer and gastrointestinal diseases; cellular movement; cell cycle and connective tissue development; and function responses (Figure 3F).

Canonical Pathway and Network Analysis

To understand the functional annotations and molecular interactions of the DEGs, a canonical pathway and network analysis were performed. Pathway analysis for the DEGs in the cells exposed to 10 µg/mL CdTe-QDs for 6 h showed *RhoA*, *eIF2* and *FAK* signaling, hepatic fibrosis, and virus entry via endocytic pathways as the significantly ($P < 0.05$) affected pathways (Figure 4A). *RhoA* and integrin signaling, regulation of the epithelial-mesenchymal transition pathway, virus entry via endocytic pathways, and cell cycle G1/S checkpoint regulation were found to be significantly upregulated in the cells exposed to the higher dose of 25 µg/mL CdTe-QDs for 6 h (Figure 4B).

Figure 4C reveals the significantly associated pathways with the DEGs in cells treated with 10 µg/mL CdTe-QDs for 12 h, and these include osteoarthritis, agrin interactions of the neuromuscular junction, gluconeogenesis I, cleavage and polyadenylation of pre-mRNA, and dermatan sulphate degradation pathways. Similarly, for the same duration (i.e. 12 h), a higher dose of 25 µg/mL of CdTe-QDs resulted in ATM and HIPPO signaling, the role of PKR in interferon induction and antiviral response, unfolded protein response, and cell cycle G2/M damage check-point regulation pathway enrichment (Figure 4D). In conducting biosynthesis of heme from uroporphyrinogen,

Paxillin, and Ga12/13 signaling, prostanoid and heme biosynthesis pathways were observed to be significantly enriched in cells treated with 10 µg/mL of CdTe-QDs for 24 h (Figure 4E). Furthermore, analysis of DEGs in cells treated with CdTe-QDs (25 µg/mL for 24 h) revealed activities of pathways, including unfolded protein response, cholesterol biosynthesis I, II, and III, and dermatan sulphate degradation responses (Figure 4F).

The most significant gene-to-gene interaction network generated for the DEGs in the treatment group 10 µg/mL for 6 h is shown in Figure 5A. We observed that there was upregulation of 24 genes (*RAB35*, *CSNK1A1*, *AKT2*, *EEF1E1*, *SRSF5*, *SRSF4*, *SRSF3*, *WTAP*, *MRTO4*, *AIMP2*, *RBM25*, *GAS5*, *MALAT1*, *NRG*, *TM9SF3*, *ELF1*, *FBXO11*, *DOK3*, *AMD1*, *XPO7*, *HEATR3*, *C9ORF3*, *MIOS*, and *FKBP15*) and downregulation of 10 genes (*CDK18*, *Alcohol Group Acceptor phosphotransferase*, *PKN1*, *SH3PXD2B*, *SORBS2*, *HIFX*, *KLHL24*, *EGFR*, *Phosphatidylinositol-4,5- bisphosphate 3-kinase* and *PLEKHG2*). In the Chang cancer cells treated with 25 µg/mL of CdTe-QDs for 6 h, high expression of 25 genes (*TRA2B*, *SAFB*, *LUC7L2*, *SRRT*, *WTAP*, *SRSF3*, *SRSF4*, *SRSF5*, *SRSF6*, *SRSF7*, *SRSF8*, *TRA2A*, *MRPS15*, *NFX1*, *RAB14*, *CBFB*, *SMURF2*, *ERM*, *RAB2A*, *ATF6B*, *GFMI*, *ELK4*, *ARHGAP35*, *AP15*, and *PMCH*) was observed. However, only 8 genes (*ICAM5*, *ARHGAP5*, *RHOGAP*, *LDLRAD4*, *MAG13*, *NLGN2*, *DLX3*, and *CGA*) exhibited low expression (Figure 5B). In contrast to 6 h exposure, network analysis for cells treated with 10 µg/mL of CdTe-QDs for 12 h depicts 7 upregulated genes (*NAA50*, *IDS*, *YTHDF3*, *PHAX*, *NOL7*, *SP100* and *USP31*) and 26 downregulated genes (*SCAF11*, *BCOR*, *B3GALNT2*, *CALU*, *NBPF10*, *LETMD1*, *ORMDL1*, *MYO1G*, *FOS*, *NACA*, *PNISR*, *RPL10*, *MALAT1*, *RPS24*, *L3MBTL1*, *SFPQ*, *PAN2*, gene for 60 S ribosomal subunit, *CBX3*, *HP1*, *NR2C1*, *HNRNPA3*, *DUB*, *RPL37A*, *RPL37* and *USP34*) (Figure 5C).

Network analysis of cells exposed to CdTe-QDs (25 µg/ml) for 12 h exposure revealed a significant network of gene interaction, which included 20 genes that were upregulated (*IGF2BP3*, *DICER1*, *RBM25*, *SMCHD1*, *SMN1/SMN2*, *SFPQ*, *KHDRBS1*, *DHX9*, *EWSR1*, *ZNF184*, *ZNF383*, *CRY1*, *DCUN1D1*, *FUS*, *YWHAH*, *AKIRIN1*, *ABI1*, *PIK3R1*, *KCTD5*, and *NEK1*), and 15 genes that were downregulated (*GREB1 L*, *OBSL1*, *HNRNPR*, *SLC38A5*, *TMEM261*, *HNRNPD*, *CUTA*, *IMMP2 L*, *SYNCRIP*, *PKM*, *TLN1*, *GOPC*, *CYFIP1*, *CCDC88A*, and *KIAA0930*) (Figure 5D). Furthermore, in cells treated with 10 µg/mL of CdTe-QDs for 24 h, 7 genes were significantly overexpressed (*F2RL2*, *PPIA*, *ZNF83*, *DHX9*, *MT1F*, *MT1E*, and *RSAD2*), whereas 7 genes were suppressed (*ITGB4*, *PTGS1*, *PTK2*, *PHLDA1*, *FAK-SRC*, *TXNIP*, and *HSPA6*) (Figure 5E). Figure 5F shows upregulation of 12 genes (*SLC7A6OS*, *MAP4K4*, *SNAI2*, *GNAS*, *KYAT1*, *RIMKLB*, *NXF1*, *DDX59*, *METTL5*, *EED*, *ANKRD33B*, and *NAA25*) and downregulation of 22 genes (*ALG14*, *ALG9*, *IQSEC2*, *SAMD4B*, *MAGED2*, *ILK*, *ST6GALNAC4*, *SLC35B4*, *TMEM141*, *RAB5C*, *MEX3D*, *SNCA*, *VAPA*, *DPY19L4*, *MEGF8*, *PCYOX1 L*, *ALG1*, *TMEM117*, *DCAKD*, *GNAI2*, *SLC39A9* and *APMAP*) in the cells treated with 25 µg/mL of

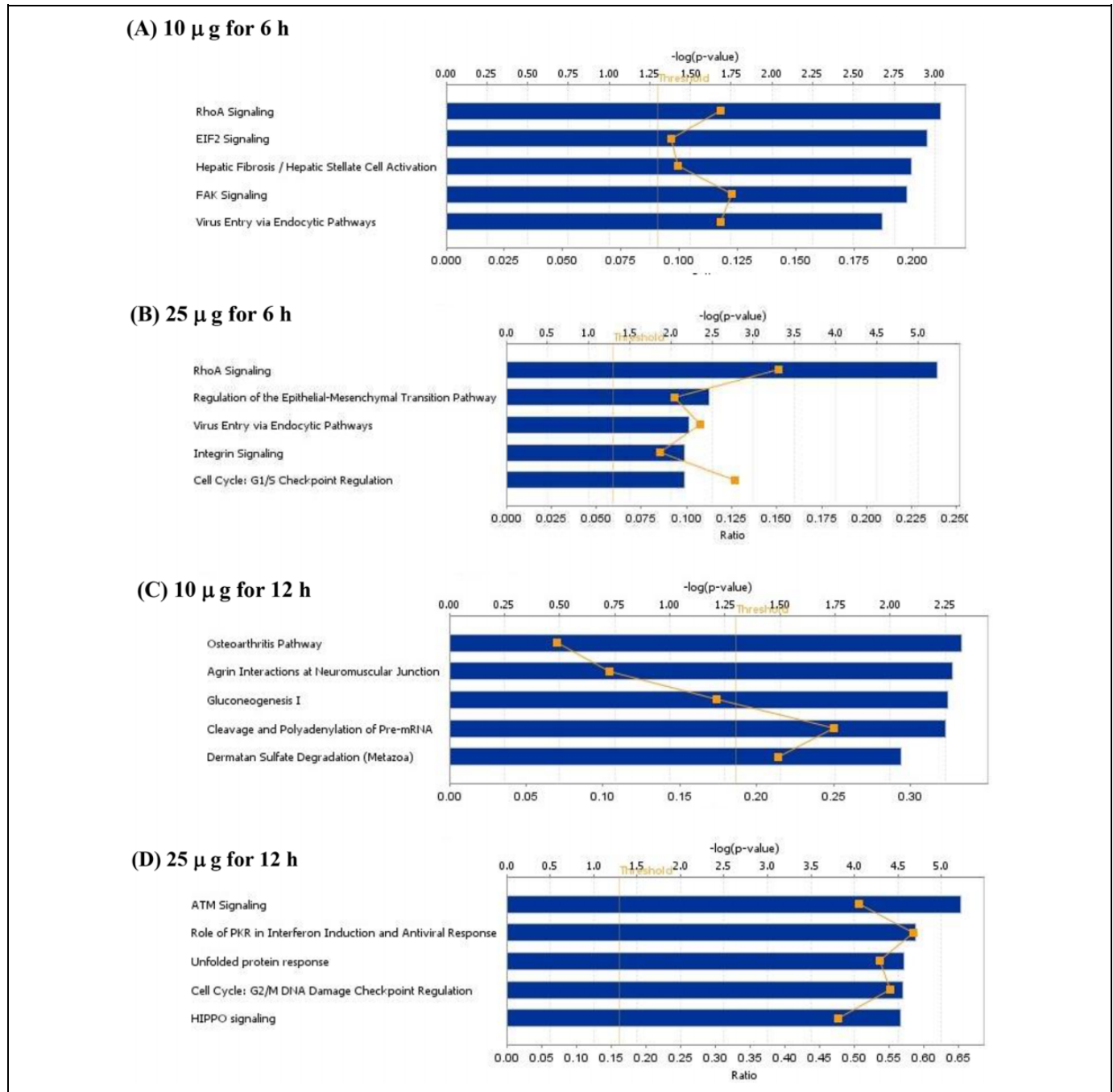


Figure 4. Canonical pathways of DEGs that are significant in 10 μ g and 25 μ g at 6 h. X-axis indicates the significance ($-\log_{10}(P\text{-value})$). The threshold line represents a P value of 0.05. For 10 μ g/mL CdTe-QDs at 6 h, *RhoA*, *elf2* and *FAK* signaling, hepatic fibrosis and endocytic pathways are the significantly ($P < 0.05$) affected pathways (A). For 25 μ g/mL CdTe-QDs at 6 h, *RhoA* and integrin signaling, EMT pathway, endocytic pathways and cell cycle G1/S checkpoint regulation were upregulated (B). For 10 μ g/mL CdTe-QDs at 12 h, significantly associated pathways included osteoarthritis, agrin interactions of neuromuscular junction, gluconeogenesis I, cleavage and polyadenylation of pre-mRNA and dermatan sulphate degradation pathways (C). For 25 μ g/mL of CdTe-QDs at 12 h, *ATM* and *HIPPO* signaling, role of *PKR* in interferon induction and anti-viral response, unfolded protein response, and cell cycle G2/M damage check-point regulation pathways were enriched (D). For 10 μ g/mL CdTe-QDs at 24 h, biosynthesis from uroporphyrinogen, Paxillin and Ga12/13 signaling, prostanoid and heme biosynthesis pathways were significantly enriched (E). For 25 μ g/mL at 24 h, pathways associated with unfolded protein response, cholesterol biosynthesis I, II and III, and dermatan sulphate degradation responses were highlighted (F).

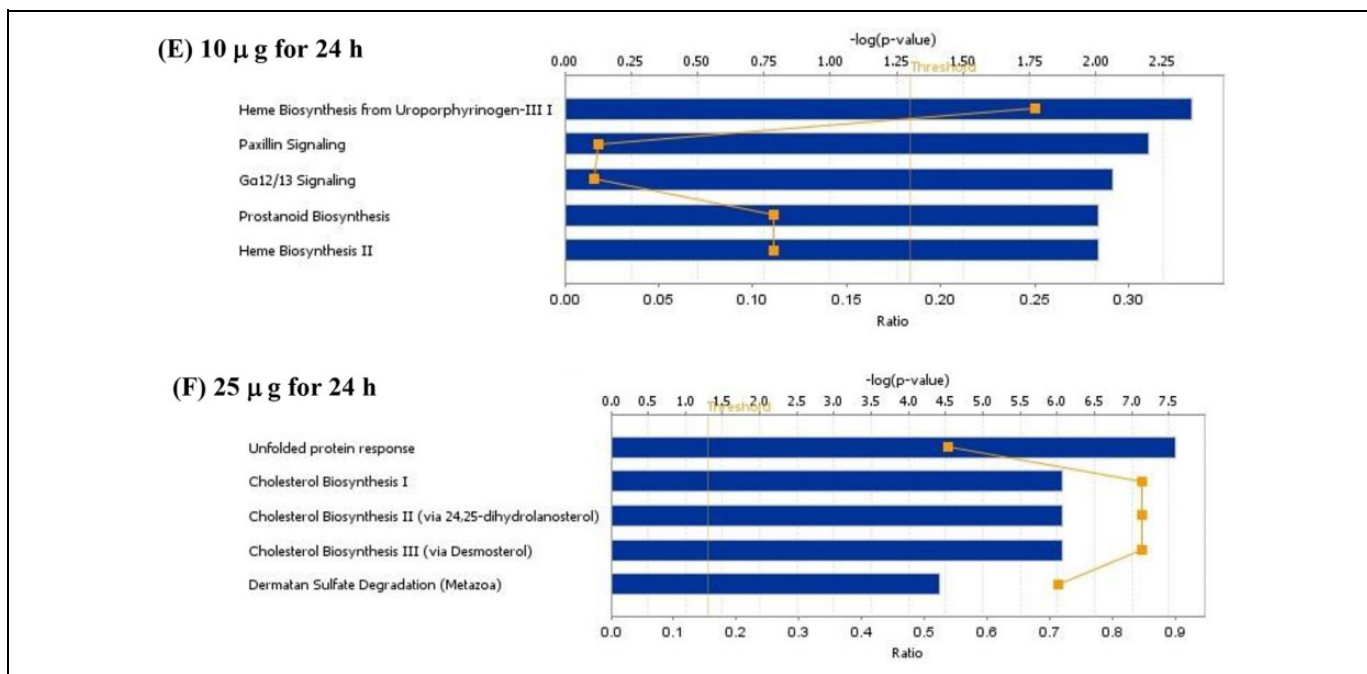


Figure 4. (continued).

CdTe-QDs for 24 h (see Figure 5F). Taken together, it appears that cells exposed to the high-dose of CdTe-QDs for 12 h and 24 h exhibited reduced responsiveness with respect to the number of genes whose expression levels were influenced when compared to the cells exposed to the low dose CdTe-QDs (Figures 5D and 5F).

Validation of Differential Gene Expression via Quantitative RT-PCR

To confirm the effect of the CdTe-QD exposure to the cells on the observed gene expressions above, the transcriptional changes in some of these genes were further confirmed by quantitative PCR (qPCR) (Figure 6), and genes that were most responsive to CdTe-QD treatment were presented as having the highest fold change in transcriptional expression. From the cells exposed to 10 µg/ml of CdTe-QDs, expression of *MCL1* and *PTPN12* at 6 h, *BRMS1L*, *IF27* and *CHM* at 12 h and *UROD*, *MTIE*, and *NUDT12* at 24 h were found to be upregulated when compared with the control unexposed cells. For cells exposed to 25 µg/ml of CdTe-QDs, expressions of *SRF6* and *RBM14* at 6 h, and *CXCL11*, *GBP1*, and *EGR1* at 12 h were upregulated. No gene was found to be upregulated at 24 h (Figure 6A). Of the genes upregulated, *CXCL11*, *GBP1*, and *EGR1* had a more than 100-fold expression level compared with the unexposed control. Of the genes that were downregulated, *TXNP*, *IFI44L*, and *VLDLR* were observed in cells exposed to 10 µg/ml CdTe-QDs for 6 h, *MIR21*, *N4BP2L2* and *PTGS1* at 12 h, and *PTK2* at 24 h. However, for cells exposed to 25 µg/ml of CdTe-QDs, *MRI* and *FASN* at 6 h, *METTL7A*

and *DEPDC1* at 12 h, and *GSTM4* and *DHCR7* at 24 h were the observed downregulated genes (Figure 6B).

Discussion

Various studies have examined the toxic effects of CdTe-QDs on human hepatocellular carcinoma HepG2 cells², human breast cancer MCF-7 cells,²³ the NIH 3T3 mouse embryo fibroblast cell line,²⁴ rat pheochromocytoma PC12 cells, and murine microglial N9 cells.²⁵ As CdTe-QDs have potential application in cancer treatment, it is pertinent to investigate the influence of these particles on cancer progression. Here, we evaluated the impact of CdTe-QDs on further activation of cancer pathways using Chang cancer cells. Our data revealed various differentially expressed genes (DEGs), which are involved in various biological processes, canonical pathways, and networks, with possible contributions to oncogenesis. The Chang cancer cell line is a mild cancer cell line with moderate oncogenic tendencies,²⁶ making it the perfect cell model to study the effect of CdTe-QDs on aggravation of neoplastic tendencies of a cancer cell. We also assessed the effect of naked/pristine CdTe-QDs (i.e. without polymer coating) on a Chang cancer cell line in a concentration- and time-dependent manner via microarray analysis. 'Naked' CdTe-QDs are generated within the cells due to the degradation of the outer shield and are responsible for injury to the exposed cells.^{10,13} Interestingly, based on previous reports, CdTe-QDs do not often yield a dose-dependent effect, making them interesting to study. A previous study has established that treatment with 25 µg/mL of CdTe-QDs for 48 h causes severe changes in cellular morphology and a less than 50% reduction in reduced cell viability of HuH-7 cells.

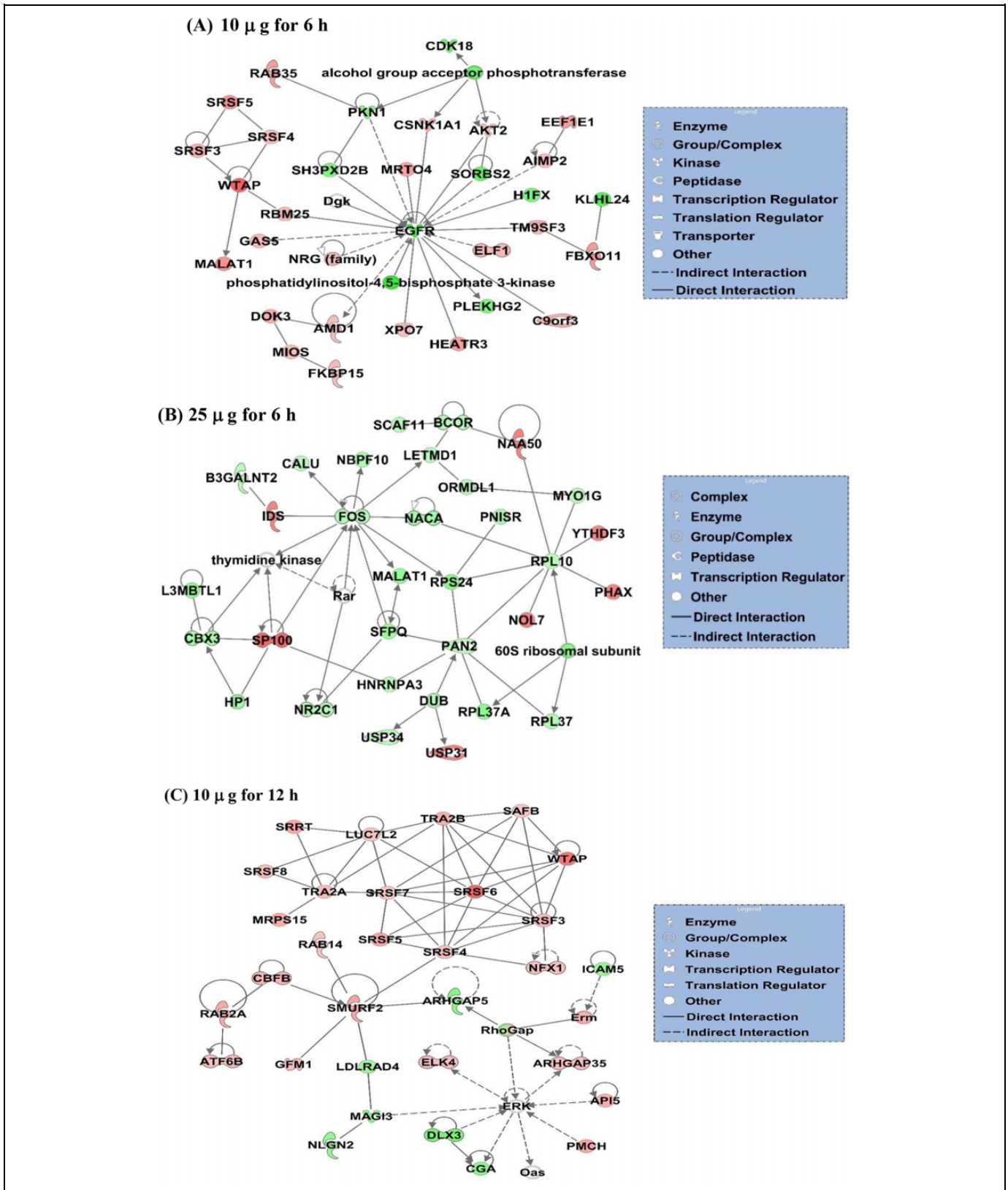


Figure 5. Top significant subnetworks of DEGs that are significant for 10 µg and 25 µg at 6 h. Green indicates downregulated, and red, upregulated. The colour intensity correlates with fold change. Straight and dashed lines represent direct or indirect gene-to-gene interactions respectively. The most significant gene-to-gene interaction network generated for DEGs in the treatment group 10 µg/mL for 6 h (A) and 25 µg/mL at 6 h (B), 10 µg/mL of CdTe-QDs at 12 h (C) and 25 µg/mL at 12 h (D), 10 µg/mL of CdTe-QDs at 24 h (E), and 25 µg/mL of CdTe-QDs at 24 h (F).

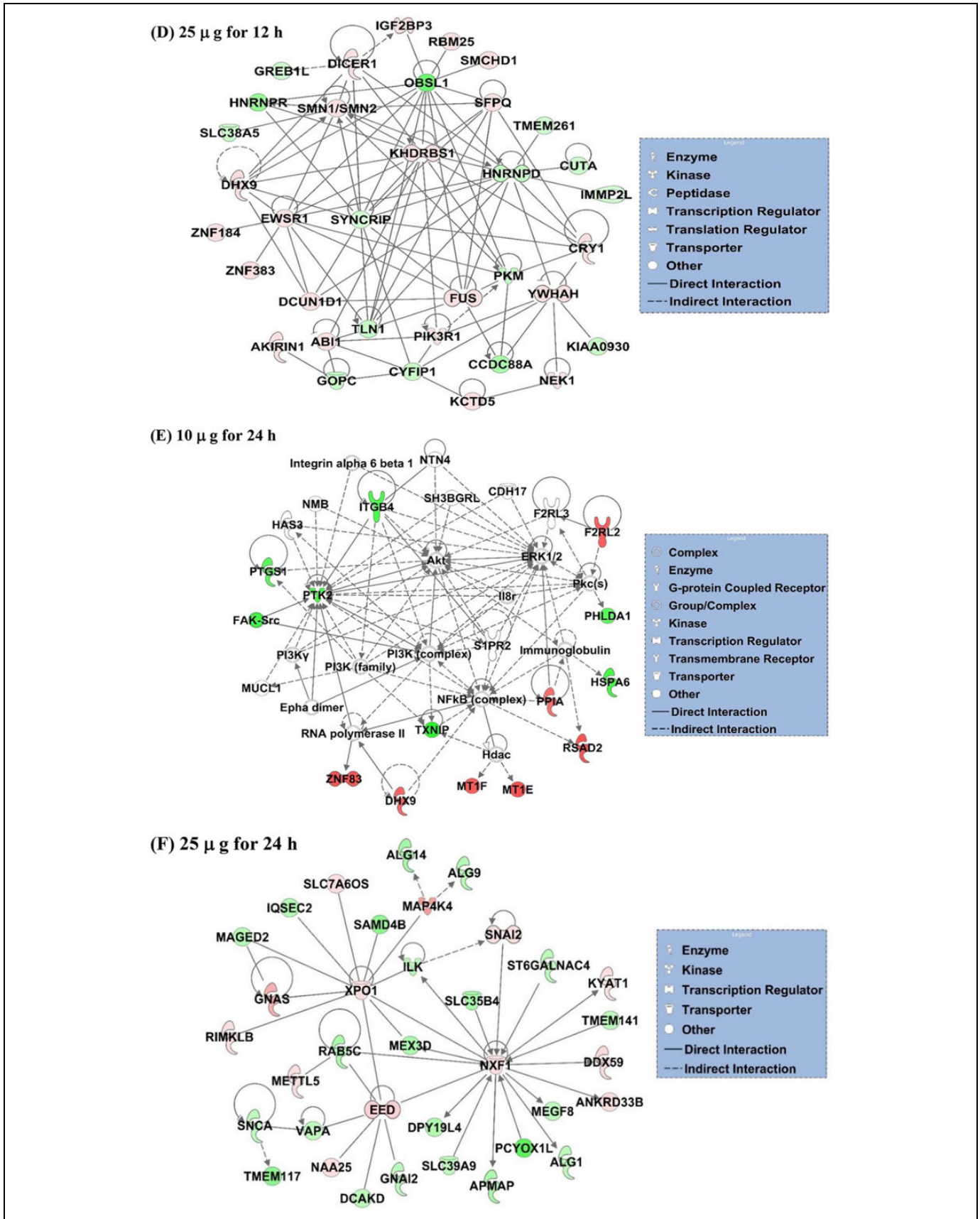


Figure 5. (continued).

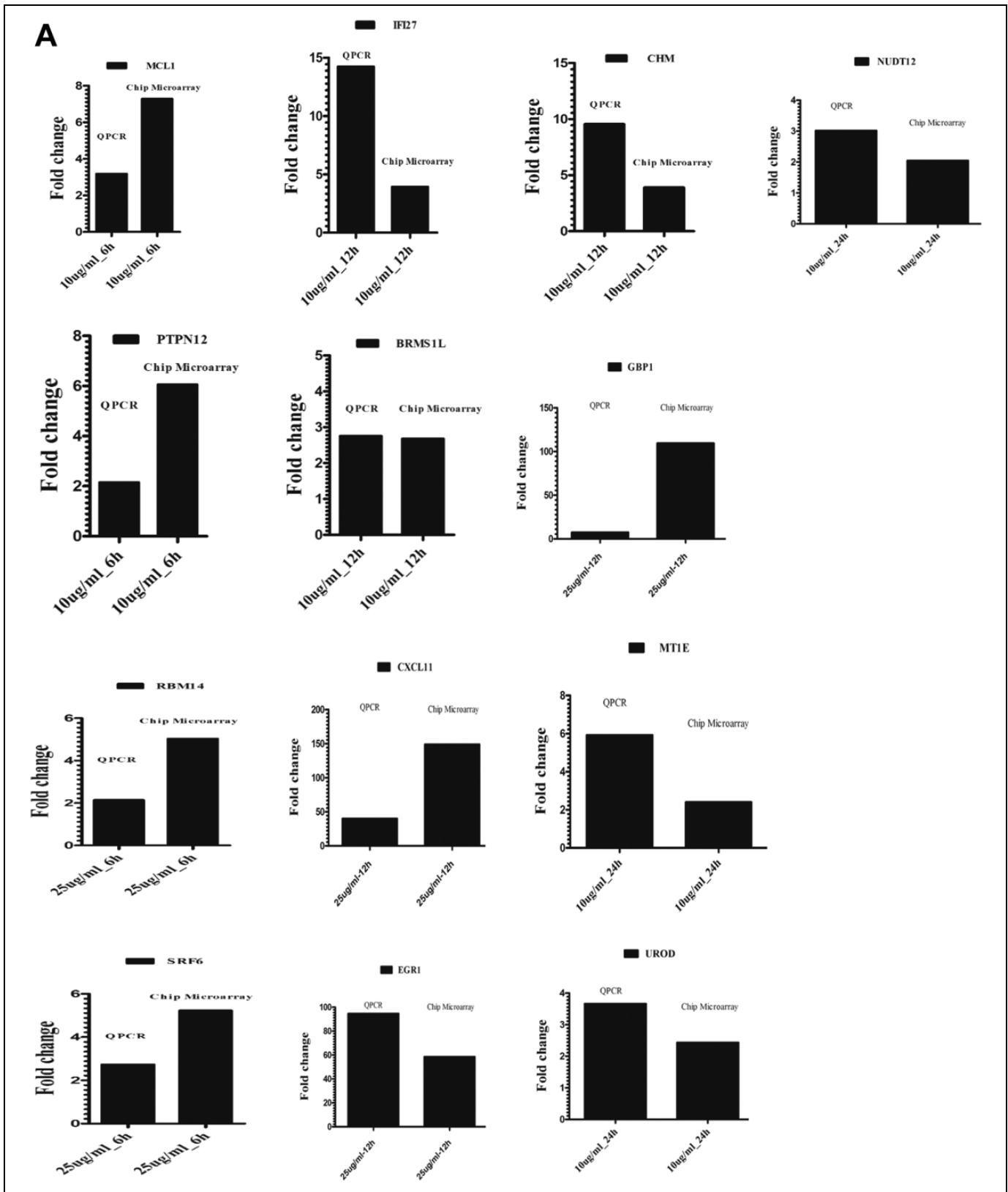


Figure 6. Quantitative RT-PCR validation of microarray gene expression. Selected genes that were significantly and differentially expressed in the microarray analysis were individually tested via qRT-PCR. Isolated RNA was treated with DNase; cDNA was synthesized. Primers and probes for the target genes were commercially procured. Taqman Universal qPCR Master Mix was used and the amplification reaction was set up. The fold-changes of the specific RNA transcripts were calculated using the ΔC_t method. The mRNA expression levels of studied genes were normalized to GAPDH. The final data for qRT-PCR are described as mean \pm standard deviation (SD) change relative to the untreated cells. **(A)** represents upregulated genes whereas **(B)** denotes downregulated target genes.

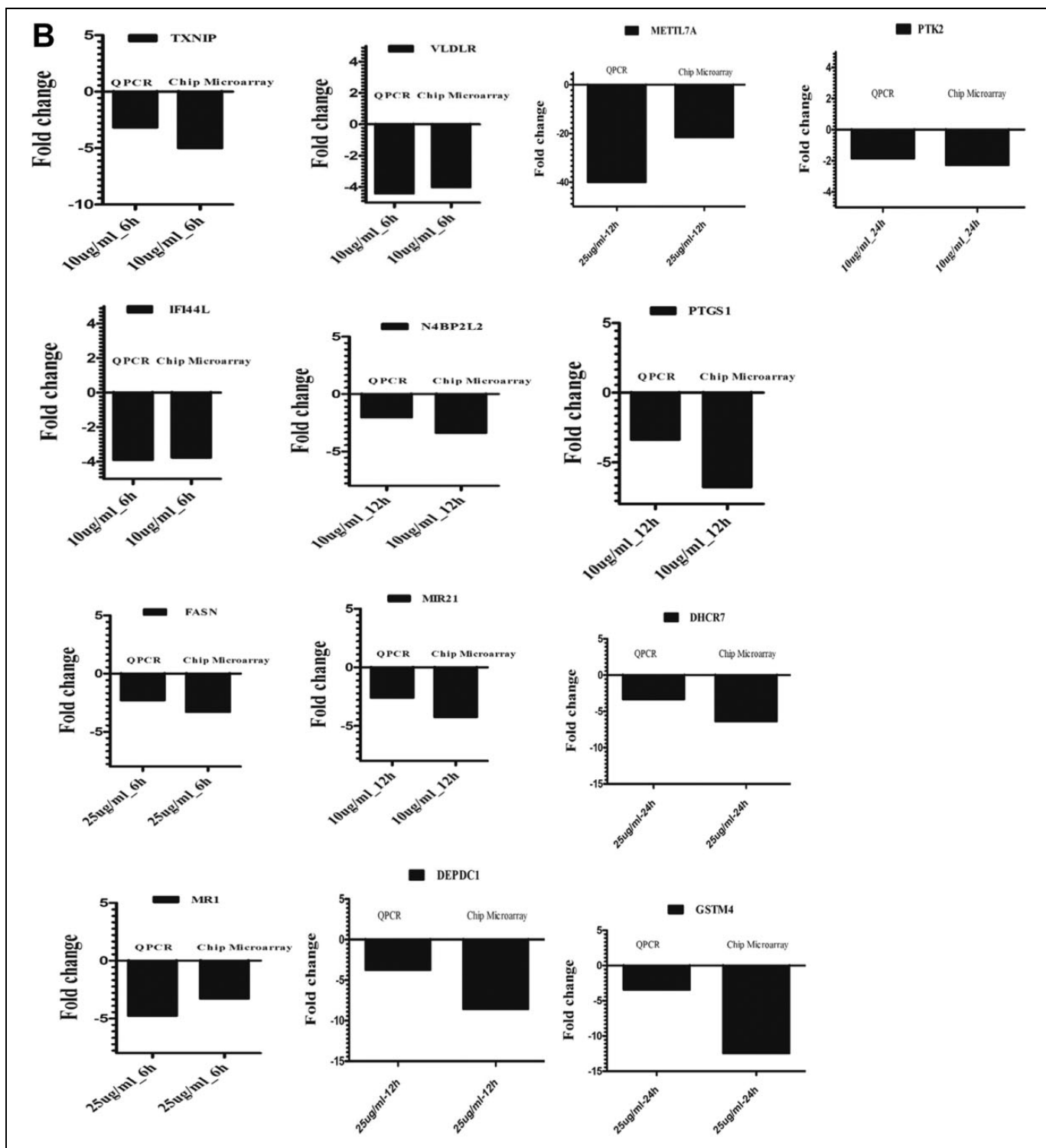


Figure 6. (continued).

However, exposure of the same cell line to a lower dose of 10 $\mu\text{g}/\text{mL}$ of CdTe-QDs causes an approximately 80% reduction in cell viability when compared to untreated HuH-7 cells (100% viable cells).¹⁶ Contrastingly, there are reports of CdTe-QDs causing toxicity in HepG2 cells in a dose- and

time-dependent manner,^{2,22} human erythroleukemia, embryonic kidney cells,²⁷ and the human breast cancer cell line.¹⁰

In this study, we identified 10,575 and 1891 genes as DEGs in the Chang cancer cells exposed to 10 and 25 $\mu\text{g}/\text{mL}$ of CdTe-QDs respectively. Treatments with a high dose of CdTe-QDs

induced the maximum activation of genes (7644 genes) at 12 h. Of these genes, and based on the results of microarray analyses, the genes with the highest fold change in the transcriptional level represent the most responsive genes to CdTe-QD exposure. To validate these findings, key genes from the microarray analysis were validated via qPCR analysis. CdTe-QDs (25 µg/ml) placed on Chang cancer cells caused maximum fold change at the transcriptional level of *CXCL11* and *GBP1* (150 and 110 folds respectively) at 12 h. *CXCL11* encodes CXCL11—a chemokine that has been implicated in bronchial inflammation, adaptive immune responses to tumours, and viral infections.^{28,29} In addition, *CXCL11* is known to control tumour growth as well as the metastatic tendencies of tumour cells, and its upregulation has been reported in tumour cells derived from colorectal cancer patients.^{28,30} Downregulation of *CXCL11* has been demonstrated to inhibit colorectal cancer cell growth and metastasis *in vivo*.³⁰ *GBP1* (115-fold change) and early growth response 1 (*EGR1*) genes were highly expressed. *GBP1* encodes GBP1 (Guanylate Binding Protein 1) – a protein that is known to be upregulated in autoimmune diseases, inflammatory bowel diseases (IBD), and some cancers.³¹ Furthermore, *EGR1* encoding early growth response 1 (*EGR1*), a transcriptional factor involved in cell proliferation and apoptosis regulation,³² was found to be highly upregulated in this study. *EGR1* is involved in different oncogenic processes and has been documented to be highly expressed in prostate cancer.³³ Other upregulated genes were *CHM*, *IFI27*, *MCL1*, *PTPN12*, *MTIE*, and *UROD*, all of which have been reported to be involved in carcinogenesis.^{34–38} For instance, *MTIE* is a methallothionein protein that is involved in myoepithelial cell differentiation, tumour cell invasiveness, and cell migration, thus promoting cancer development and progression.^{39,40}

Several downregulated genes were observed in the qPCR confirmatory tests, and those with the highest fold of gene expression downregulation, such as *METTL7A* and *TXNIP*, showed consistency with the findings of other studies. *METTL7A* is a gene encoding methyl-transferase-like 7A (*METTL7A*) protein, which likely functions as a tumour suppressor, as its expression is known to be downregulated in different cancers such as thyroid cancer.^{41,42} Another study also reported that downregulation of *METTL7A* favours tumor progression.⁴³ *GSTM4*, another gene known to be involved in oncogenic transformation,⁴⁴ was downregulated by >12-fold. Other genes found to be downregulated are associated with metabolism (*DHCR7*, *FASN*), transcription regulation (*DEPDC1*, *MIR21*, *N4BP2L2*), and signaling pathways (*PTK2*, *VLDLR*). When taken together, these findings show that the genes found to be highly expressed in response to CdTe-QD exposure are linked with immune responses and are also potential contributors to tumorigenesis. In contrast, genes that were downregulated, function in pathways involved in protein synthesis, metabolism, and tumour suppression. As depicted in the Venn diagrams displayed in this paper, only 7 genes were expressed in response to 10 µg/mL of CdTe-QDs, while a higher number of genes were found to be activated when

expressed with 25 µg/mL of CdTe-QDs. Although DEGs by CdTe-QDs were distinct at different time points, a set of DEGs represented a general response of the Chang cancer cells to CdTe-QDs, consistent with observations made for TiO₂ nanobelts and carbon nanotubes.⁴⁵ The GO analysis showed significant enhancement of several biological processes, including cell cycle, cell death and survival, cell growth and proliferation responses, gene expression, developmental responses, cell-to-cell signaling, nucleic acid metabolism, and responses to cancer. Studies involving microRNAs in cadmium telluride (CdTe) nanomaterial cytotoxicity also reported upregulation of GO processes, related to cell proliferation, development, growth, and apoptosis.⁴⁶

Network analyses for pathway activation showed that the RAS pathway was significantly activated due to CdTe-QD exposure. The RAS member, RhoA, regulates cell migration and cell cycle progression⁴⁷ and innate immune response via eukaryotic Initiation Factor 2 (*eIF2*) signaling.⁴⁸ The RAS pathway is strongly modulated in HepG2 cells,⁴⁹ liver injury, and chronic liver diseases.^{50,51} Furthermore, activation of integrin and focal adhesion kinase (FAK) signaling pathways, as observed here, suggests regulation of cell migration, cell proliferation, and angiogenesis, all of which are known to contribute to carcinogenesis in different cell types.^{52–54} Genes involved in epithelial-mesenchymal transition (EMT) and G1/S checkpoint regulatory pathways were also noticeably upregulated, highlighting the potential for fibrosis, cancer progression⁵⁵ and oncogenesis.⁵⁶

CdTe-QD treatment can cause DNA damage^{7,57}: we found increased levels of ataxia telangiectasia-mutated (*ATM*) signaling pathway, crucial for the cellular responses to DNA damage response and repair.⁵⁸ Another canonical pathway enriched by DEGs upon CdTe-QD exposure was the unfolded protein response (UPR) pathway. The UPR pathway is a pro-survival pathway that is activated in response to cellular stress and metabolism to re-establish homeostasis and maintain survival, thereby contributing to cancer development and progression.⁵⁹ Additionally, upregulation of paxillin and Gα12/13 signaling pathways were observed, and this has been implicated in cell proliferation in prostate cancer⁶⁰ and cell migration/invasiveness⁶¹ respectively.

The network of DEGs in cells exposed to 10 µg/mL CdTe-QDs for 6 h showed upregulation of genes associated with cell proliferation, gene expression, metabolism and signal transduction. The DEGs exposed for 12 h included downregulated genes that are transcription factors, and those that are members of the *Fos* family of proteins associated with signal transduction and cell proliferation. The decreased expression of *Fos* has been reported to be associated with tumour progression in several types of cancers.^{62,63} Another upregulated gene, *RSAD2*, encodes a well-known anti-viral response protein, which is known to be overexpressed when cells are exposed to iron nanoparticles.^{64,65} At 24 h, CdTe-QDs were found to upregulate *MAP4K4*, which encodes MAP4K4 and belongs to the Mitogen Activated Protein Kinase family. MAP4K4 is involved in signal transduction, cell proliferation and migration, and it is overexpressed in carcinoma cells.⁶⁶ Another gene

found to be overexpressed is *SNAI2*, which encodes a zinc-finger transcription factor that has been shown to have anti-apoptotic activity, enhancing the survival ability of tumour cells. This gene is upregulated in different types of cancers.⁶⁷

Interestingly, several pathways related to viral infection (virus entry via the endocytic pathway and hepatic fibrosis pathway) were significantly enriched by the DEGs, and have also been reported to be active in neurotoxicity in rats⁸ and cells exposed to iron nanoparticles.^{20,68} Based on the gene expression pattern observed in the gene interaction and network analysis, it appears that genes responsible for induction of the immune response, cell adhesion and migration, type I interferon signaling pathway, cell proliferation, endoplasmic reticulum stress, and unfolded protein response were significantly induced. These biological and cellular processes are required for cancer development and tumorigenesis. For example, immune modulation is employed by cancer cells to evade the host immune response or to augment the host's immune response to facilitate the growth of cancer cells.⁶⁹ Similarly, cell migration determines the metastatic potential of different cancer cells. Cells that overexpress genes responsible for cell migration are characterized by an aggressive form of cancer.⁷⁰ Pathways that include cell cycle progression and G2/M DNA damage checkpoint regulation were also upregulated. One of the hallmarks of cancer is an evasion of DNA damage repair and uncontrolled progression through the cell cycle, which increases the accumulation of mutation, and cancer development and progression.⁷¹ Thus, CdTe-QDs may exert an oncogenic influence on Chang cancer cells, which may also enhance the oncogenic potential of Chang cancer cells, thus driving cancer progression and tumorigenesis and lending support to the oncogenic implications of Cd-containing QDs.⁶⁷⁻⁶⁹

In conclusion, CdTe-QD exposure to Chang cancer cells triggered differential expression of genes in a dose- and time-dependent manner. Furthermore, many DEGs regulated by CdTe-QDs influence transcriptional processes, biological processes, canonical pathways, and network interactions that are associated with oncogenic transformation or cancer progression.

Authors' Note

The data used to support the findings of this study are available from the corresponding author upon request.

Acknowledgments

The authors would like to thank the Research Centre administration at King Faisal Specialist Hospital & Research Centre for their support. The authors would also like to thank Dr. Azeez Oriyomi Yusuf for his assistance in the language editing of the manuscript.

Author Contributions

Conceptualization, Ahmed Al-Qahtani; Data curation, Dilek Colak, Salma Wakil and Samya Hagos; Formal analysis, Dilek Colak; Investigation, Mashael Al-Anazi, and Marie Fe Bohol; Methodology, Mohammed Aldughaim, Salma Wakil, Samya Hagos, Sashmita Rout, and Ahmed Al-Qahtani; Project administration, Mohammed Al-Ahdal and Ahmed Al-Qahtani; Resources, Daoud Ali, Saud Alarifi and Saad Alkahtani; Software, Hani Alotheid and Ahmed Al-Qahtani; Supervision, Daoud Ali, Saud Alarifi and Saad Alkahtani; Validation, Mashael

Al-Anazi, Marie Fe Bohol and Ahmed Al-Qahtani; Writing-original draft, Mohammed Aldughaim, Saud Alarifi, Mohammed Al-Ahdal and Ahmed Al-Qahtani; Writing-review & editing, Marie Fe Bohol, Hani Alotheid, Daoud Ali, Sashmita Rout and Saad Alkahtani. All authors have read and agreed to the submitted version of the manuscript.


Declaration of Conflicting Interests


The author(s) declared no potential conflicts of interest with respect to the research, authorship, and/or publication of this article.


Funding


The author(s) received no financial support for the research, authorship, and/or publication of this article.

ORCID iDs

Marie Fe F. Bohol  <https://orcid.org/0000-0003-1981-2327>

Dilek Colak  <https://orcid.org/0000-0001-6485-8768>

Hani Alotheid  <https://orcid.org/0000-0003-0132-558X>

Saud Alarifi  <https://orcid.org/0000-0002-3613-5228>

Supplemental Material

Supplemental material for this article is available online.

References

1. Valizadeh A, Mikaeili H, Samiei M, et al. Quantum dots: synthesis, bioapplications, and toxicity. *Nanoscale Res Lett.* 2012;7(1):480.
2. Nguyen KC, Willmore WG, Tayabali AF. Cadmium telluride quantum dots cause oxidative stress leading to extrinsic and intrinsic apoptosis in hepatocellular carcinoma HepG2 cells. *Toxicology.* 2013;306:114-123.
3. Zrazhevskiy P, Sena M, Gao X. Designing multifunctional quantum dots for bioimaging, detection, and drug delivery. *Chem Soc Rev.* 2010;39(11):4326-4354.
4. Jaiswal JK, Simon SM. Potentials and pitfalls of fluorescent quantum dots for biological imaging. *Trends Cell Biol.* 2004;14(9):497-504.
5. Hardman R. A toxicologic review of quantum dots: toxicity depends on physicochemical and environmental factors. *Environ Health Perspect.* 2006;114(2):165-172.
6. Ung Thi Dieu T, Toan PS, Chi TTK, Khang DD, Liem NQ. CdTe quantum dots for an application in the life sciences. *Adv Nat Sci: Nanosci Nanotechnol.* 2010;1(4):045009.
7. Chen H, Gong Y, Han R. Cadmium telluride quantum dots (CdTe-QDs) and enhanced ultraviolet-B (UV-B) radiation trigger anti-oxidant enzyme metabolism and programmed cell death in wheat seedlings. *PLoS One.* 2014;9(10):e110400.
8. Wu T, He K, Ang S, et al. Impairments of spatial learning and memory following intrahippocampal injection in rats of 3-mercaptopropionic acid-modified CdTe quantum dots and molecular mechanisms. *Int J Nanomedicine.* 2016;11:2737-2755.
9. Wu D, Lu J, Ma Y, Cao Y, Zhan T. Mitochondrial dynamics and mitophagy involved in MPA-capped CdTe quantum dots-induced toxicity in the human liver carcinoma (HepG2) cell line. *Environ Pollut.* 2020;274:115681.
10. Lovrić J, Cho SJ, Winnik FM, Maysinger D. Unmodified cadmium telluride quantum dots induce reactive oxygen species

- formation leading to multiple organelle damage and cell death. *Chem Biol*. 2005;12(11):1227-1234.
11. Akhavan O, Hashemi E, Zare H, Shamsara M, Taghavinia N, Heidari F. Influence of heavy nanocrystals on spermatozoa and fertility of mammals. *Mater Sci Eng: C*. 2016;69:52-59.
 12. Ambrosone A, Mattera L, Marchesano V, et al. Mechanisms underlying toxicity induced by CdTe quantum dots determined in an invertebrate model organism. *Biomaterials*. 2012;33(7):1991-2000.
 13. Zheng W, Xu Y-M, Wu D-D, et al. Acute and chronic cadmium telluride quantum dots-exposed human bronchial epithelial cells: The effects of particle sizes on their cytotoxicity and carcinogenicity. *Biochem Biophys Res Commun*. 2018;495(1):899-903.
 14. Aghebati-Maleki A, Dolati S, Ahmadi M, et al. Nanoparticles and cancer therapy: Perspectives for application of nanoparticles in the treatment of cancers. *J Cell Physiol*. 2020;235(3):1962-1972.
 15. Ma DD, Yang WX. Engineered nanoparticles induce cell apoptosis: potential for cancer therapy. *Oncotarget*. 2016;7(26):40882-40903.
 16. Lunova M, Prokhorov A, Jirsa M, et al. Nanoparticle core stability and surface functionalization drive the mTOR signaling pathway in hepatocellular cell lines. *Sci Rep*. 2017;7(1):16049.
 17. Fang M, Peng CW, Pang DW, Li Y. Quantum dots for cancer research: current status, remaining issues, and future perspectives. *Cancer Biol Med*. 2012;9(3):151-163.
 18. Asare N, Duale N, Slagsvold HH, et al. Genotoxicity and gene expression modulation of silver and titanium dioxide nanoparticles in mice. *Nanotoxicology*. 2016;10(3):312-321.
 19. Lee SJ, Yum YN, Kim SC, et al. Distinguishing between genotoxic and non-genotoxic hepatocarcinogens by gene expression profiling and bioinformatic pathway analysis. *Sci Rep*. 2013;3:2783.
 20. Zhang L, Wang X, Zou J, Liu Y, Wang J. Effects of an 11-nm DMSA-coated iron nanoparticle on the gene expression profile of two human cell lines, THP-1 and HepG2. *J Nanobiotechnology*. 2015;13(1):3.
 21. Iyer VR, Eisen MB, Ross DT, et al. The transcriptional program in the response of human fibroblasts to serum. *Science*. 1999;283(5398):83-87.
 22. Katubi KM, Alzahrani FM, Ali D, Alarifi S. Dose- and duration-dependent cytotoxicity and genotoxicity in human hepatocarcinoma cells due to CdTe QDs exposure. *Hum Exp Toxicol*. 2019;38(8):914-926.
 23. Choi AO, Brown SE, Szyf M, Maysinger D. Quantum dot-induced epigenetic and genotoxic changes in human breast cancer cells. *J Mol Med (Berl)*. 2008;86(3):291-302.
 24. Li S, Wang H, Qi Y, et al. Assessment of nanomaterial cytotoxicity with SOLiD sequencing-based microRNA expression profiling. *Biomaterials*. 2011;32(34):9021-9030.
 25. Lovric J, Bazzi HS, Cuie Y, Fortin GR, Winnik FM, Maysinger D. Differences in subcellular distribution and toxicity of green and red emitting CdTe quantum dots. *J Mol Med (Berl)*. 2005;83(5):377-385.
 26. Gao Q, Wang XY, Wang XY, Fan J. Cell line misidentification: the case of the Chang liver cell line. *Hepatology*. 2011;54(5):1894-1895.
 27. Su Y, He Y, Lu H, et al. The cytotoxicity of cadmium based, aqueous phase - synthesized, quantum dots and its modulation by surface coating. *Biomaterials*. 2009;30(1):19-25.
 28. Kistner L, Doll D, Holtorf A, Nitsche U, Janssen KP. Interferon-inducible CXC-chemokines are crucial immune modulators and survival predictors in colorectal cancer. *Oncotarget*. 2017;8(52):89998-90012.
 29. Boyd P, Hudgens E, Loftus JP, et al. Expressed gene sequence and bioactivity of the IFN γ -response chemokine CXCL11 of swine and cattle. *Vet Immunol Immunopathol*. 2010;136(1-2):170-175.
 30. Gao YJ, Liu L, Li S, et al. Down-regulation of CXCL11 inhibits colorectal cancer cell growth and epithelial-mesenchymal transition. *Onco Targets Ther*. 2018;11:7333-7343.
 31. Britzen-Laurent N, Lipnik K, Ocker M, et al. GBP-1 acts as a tumor suppressor in colorectal cancer cells. *Carcinogenesis*. 2013;34(1):153-162.
 32. Gitenay D, Baron VT. Is EGR1 a potential target for prostate cancer therapy? *Future Oncol*. 2009;5(7):993-1003.
 33. Baron V, Adamson ED, Calogero A, Mercola D. The transcription factor Egr1 is a direct regulator of multiple tumor suppressors including TGF β 1, PTEN, p53, and fibronectin. *Cancer Gene Ther*. 2006;13(2):115-124.
 34. Yun U-J, Sung JY, Park SY, et al. Oncogenic role of rab escort protein 1 through EGFR and STAT3 pathway. *Cell Death & Amp; Disease*. 2017;8:e2621.
 35. Suomela S, Cao L, Bowcock A, Saarialho-Kere U. Interferon alpha-inducible protein 27 (IFI27) is upregulated in psoriatic skin and certain epithelial cancers. *J Invest Dermatol*. 2004;122(3):717-721.
 36. Chen Z, Sangwan V, Banerjee S, et al. miR-204 mediated loss of Myeloid cell leukemia-1 results in pancreatic cancer cell death. *Mol Cancer*. 2013;12(1):105.
 37. Harris IS, Blaser H, Moreno J, et al. PTPN12 promotes resistance to oxidative stress and supports tumorigenesis by regulating FOXO signaling. *Oncogene*. 2013;33(8):1047.
 38. Seenivasagam RK, AK G, Ramamurthy R, Kannan MA, Rao DM. Uroporphyrinogen decarboxylase gene expression in oral squamous cell carcinomas. *J Clin Oncol*. 2013;31(15_suppl):e17002-e17002.
 39. Wu Y, Siadaty MS, Berens ME, Hampton GM, Theodorescu D. Overlapping gene expression profiles of cell migration and tumor invasion in human bladder cancer identify metallothionein E1 and nicotinamide N-methyltransferase as novel regulators of cell migration. *Oncogene*. 2008;27(52):6679-6689.
 40. Lang J, Yang N, Deng J, et al. Inhibition of SARS pseudovirus cell entry by lactoferrin binding to heparan sulfate proteoglycans. *PLoS one*. 2011;6(8):e23710.
 41. Qi L, Song Y, Chan THM, et al. An RNA editing/dsRNA binding-independent gene regulatory mechanism of ADARs and its clinical implication in cancer. *Nucleic Acids Res*. 2017;45(18):10436-10451.
 42. Zhou S, Shen Y, Shen Y, et al. DNA methylation of METTL7A gene body regulates its transcriptional level in thyroid cancer. *Oncotarget*. 2017;8(21):34652-34660.
 43. Morrison JA, Pike LA, Sams SB, et al. Thioredoxin interacting protein (TXNIP) is a novel tumor suppressor in thyroid cancer. *Mol Cancer*. 2014;13:62.

44. Zhuo R, Kosak KM, Sankar S, et al. Targeting Glutathione S-transferase M4 in Ewing sarcoma. *Front Pediatr.* 2014;2:83.
45. Tilton SC, Karin NJ, Tolic A, et al. Three human cell types respond to multi-walled carbon nanotubes and titanium dioxide nanobelts with cell-specific transcriptomic and proteomic expression patterns. *Nanotoxicology.* 2014;8(5):533-48.
46. Sun B, Yang F, Hu FH, , Huang NP, Xiao ZD. Comprehensive annotation of microRNA expression profiles. *BMC Genet.* 2013; 14:120.
47. David M, D Petit, Bertoglio J. Cell cycle regulation of Rho signaling pathways. *Cell Cycle.* 2012;11(16):3003-10.
48. Shrestha N, Bahnan W, Wiley DJ, Barber G, Fields KA, Fields KA. Eukaryotic initiation factor 2 (eIF2) signaling regulates proinflammatory cytokine expression and bacterial invasion. *J Biol Chem.* 2012;287(34):28738-44.
49. Thai SF, Wallace KA, Jones CP, et al. Differential Genomic Effects on Signaling Pathways by Two Different CeO₂ Nanoparticles in HepG2 Cells. *J Nanosci Nanotechnol.* 2015;15(12):9925-37.
50. Brenner DA. Molecular Pathogenesis of Liver Fibrosis. *Trans Am Clin Climatol Assoc.* 2009;120:361-368.
51. Kong L, Li J, Wang J, et al. Genome-wide Transcriptional Analysis of Oxidative Stress-related Genes and Pathways Induced by CdTe aqQDs in Mice. *Nanotheranostics.* 2018;2(3):271-279.
52. Zhao X, Guan JL. Focal adhesion kinase and its signaling pathways in cell migration and angiogenesis. *Adv Drug Deliv Rev.* 2011;63(8):610-5.
53. Harburger DS, Calderwood DA. Integrin signalling at a glance. *J Cell Sci.* 2009;122(Pt 2):159-163.
54. Parsons JT, Slack-Davis J, Tilghman R, Roberts WG. Focal adhesion kinase: targeting adhesion signaling pathways for therapeutic intervention. *Clin Cancer Res.* 2008;14(3):627-632.
55. Lamouille S, Xu J, Derynck R. Molecular mechanisms of epithelial-mesenchymal transition. *Nat Rev Mol Cell Biol.* 2014;15(3):178-196.
56. Bertoli C, Skotheim JM, de Bruin RA. Control of cell cycle transcription during G1 and S phases. *Nat Rev Mol Cell Biol.* 2013; 14(8):518-528.
57. Fernández EL, Gustafson AL, Andersson M, Hellman B. Cadmium-induced changes in apoptotic gene expression levels and DNA damage in mouse embryos are blocked by Zinc. *Toxicological Sciences.* 2003;76(1):162-170.
58. Kitagawa R, Kastan MB. The ATM-dependent DNA damage signaling pathway. *Cold Spring Harb Symp Quant Biol.* 2005; 70:99-109.
59. Bravo R., Parra V, Gatica D, et al. Endoplasmic reticulum and the unfolded protein response: dynamics and metabolic integration. *Int Rev Cell Mol Biol.* 2013;301:215-290.
60. Sen A, De Castro I, Defranco DB, et al. Paxillin mediates extranuclear and intranuclear signaling in prostate cancer proliferation. *J Clin Invest.* 2012;122(7):2469-2481.
61. Juneja J, Casey PJ, Role of G12 proteins in oncogenesis and metastasis. *Br J Pharmacol.* 2009;158(1):32-40.
62. Kustikova O, Kramerov D, Grigorian M, et al. Fra-1 induces morphological transformation and increases in vitro invasiveness and motility of epithelioid adenocarcinoma cells. *Mol Cell Biol.* 1998;18(12):7095-7105.
63. Mahner S, Baasch C, Schwarz J, et al. C-Fos expression is a molecular predictor of progression and survival in epithelial ovarian carcinoma. *Br J Cancer.* 2008;99(8):1269-1275.
64. Liu Y, Wang J. Effects of DMSA-coated Fe₃O₄ nanoparticles on the transcription of genes related to iron and osmosis homeostasis. *Toxicol Sci.* 2013;131(2):521-536.
65. Zaas AK, Chen M, Varkey J, et al. Gene expression signatures diagnose influenza and other symptomatic respiratory viral infections in humans. *Cell Host Microbe.* 2009;6(3):207-217.
66. Huo J, Qiao J-G, Han K. The expression level of gene MAP4K4 and its clinical effect in cancerous tissue of gastric carcinoma. *Biomedical Res.* 2017;28(7):2920-2925.
67. Ganesan R, Mallets E, Gomez-Cambronero J. The transcription factors Slug (SNAI2) and Snail (SNAIL) regulate phospholipase D (PLD) promoter in opposite ways towards cancer cell invasion. *Mol Oncol.* 2016;10(5):663-676.
68. Zhang L, Chen Y, Wu L, Liu Y. Effects of Iron Nanoparticles on Immune Response of Two Immunocytes Like Virus. *Nanosci Nanotechnol Lett.* 2017;9(12):1934-1946.
69. Vinay DS, Ryan EP, Pawelec G, et al. Immune evasion in cancer: Mechanistic basis and therapeutic strategies. *Semin Cancer Biol.* 2015;35(Suppl):S185-S198.
70. Guan X. Cancer metastases: challenges and opportunities. *Acta Pharm Sin B.* 2015;5(5):402-418.
71. Hanahan D, Weinberg RA. Hallmarks of cancer: the next generation. *Cell.* 2011;144(5):646-674.